Accepted manuscript, published in:

Journal of the Mechanical Behavior of Biomedical Materials 90 (2019) 284-294

https://doi.org/10.1016/j.jmbbm.2018.09.048

Fluid load support does not explain tribological performance of PVA hydrogels

Elze Porte*, Philippa Cann, Marc Masen

Tribology Group, Department of Mechanical Engineering, Imperial College London, London SW7 2AZ, UK

*corresponding author: elze.porte14@imperial.ac.uk

Keywords: fluid load support, lubrication, hydrogel, photoelastic, friction, articular cartilage

Abstract

The application of hydrogels as articular cartilage (AC) repair or replacement materials is limited by poor tribological behaviour, as it does not match that of native AC. In cartilage, the pressurisation of the interstitial fluid is thought to be crucial for the low friction as the load is shared between the solid and liquid phase of the material. This fluid load support theory is also often applied to hydrogels. However, this theory has not been validated as no experimental evidence directly relates the pressurisation of the interstitial fluid to the frictional response of hydrogels. This lack of understanding about the governing tribological mechanisms in hydrogels limits their optimised design. Therefore, this paper aims to provide a direct measure for fluid load support in hydrogels under physiologically relevant sliding conditions. A photoelastic method was developed to simultaneously measure the load on the solid phase of the hydrogel and its friction coefficient and thus directly relate friction and fluid load support. The results showed a clear distinction in frictional behaviour between the different test conditions, but results from photoelastic images and stress-relaxation experiments indicated that fluid load support is an unlikely explanation for the frictional response of the hydrogels. A more appropriate explanation, we hypothesized, is a non-replenished lubricant mechanism. This work has important implications for the tribology of cartilage and hydrogels as it shows that the existing theories do not adequately describe the tribological behaviour of hydrogels. The developed insights can be used to optimise the tribological performance of hydrogels as articular cartilage implants.

1. Introduction

1.1 Background on cartilage replacements and mimics

Articular cartilage (AC) damaged due to sports injuries or osteoarthritis often results in stiff and painful joints and can severely reduce the mobility of the patient. Finding a material that can replace the damaged tissue is highly beneficial for the treatment of these patients as it would be a less intrusive alternative for full joint replacements. Healthy AC is an outstanding tribological material as it provides both load support and low friction (Caligaris and Ateshian, 2008; McCutchen, 1962; Moore and Burris, 2017) facilitating motion over a wide range of gait conditions. Replicating this behaviour in an artificial material has proved to be a major challenge. Hydrogels are widely studied as potential cartilage replacement materials (for example (Holloway et al., 2010; Murakami et al., 2014; Parkes et al., 2015)) because of their similar physical properties to cartilage, including a biphasic (solid/interstitial fluid), porous structure and stiffness (Spiller et al., 2011). However, the tribological performance is often still lacking compared to AC (Blum and Ovaert, 2013; Li et al., 2010; Parkes et al., 2015).

Hydrogels are biphasic materials with a solid matrix made from a hydrophilic cross-linked polymer network (Hoffman, 2002). The term hydrogels covers a wide range of materials made from naturally derived or synthetic polymers, which can be either chemically or physically cross-linked (Hoffman, 2002). They can be made with similar properties to cartilage, for example its compressive and shear moduli (Spiller et al., 2011). Hydrogels can also be made with comparable permeability (Baykal et al., 2013; Spiller et al., 2011), but the pore size is often much greater (~5-40um) (Holloway et al., 2010; Parkes et al., 2015), compared to several nanometres in cartilage (Majda et al., 2017; Mow et al., 1992). Depending on whether the hydrogel is used as a short term bio-scaffold for AC cell regeneration (O'Connell et al., 2012) or longer-term permanent replacement (Holloway et al., 2010) the material must provide load carrying, low friction, and minimal wear over many millions of loading and gait cycles (Silva et al., 2002). Developing a suitable hydrogel which fulfils these properties requires a detailed understanding of the fundamental lubrication mechanisms under different loading and motion conditions. Additionally, hydrogel AC mimics can be very useful for research purposes, as they can be used as an AC model with the possibility to control and adapt their properties to study the contribution of specific properties, for example material stiffness, to the tribological behaviour.

The aim of this paper is to contribute to the development of suitable AC mimics by examining fundamental lubrication mechanisms of hydrogels as replacement materials for damaged AC. One of the major theories in AC tribology is that of fluid load support (Ateshian et al., 1998), where low friction is sustained by the continuous pressurisation of the interstitial fluid that carries part of the load. This is reported to reduce the friction of AC by up to 85% (Caligaris and Ateshian, 2008), and is therefore considered very important for AC tribology. As yet, the only direct experimental evidence for this mechanism is obtained on cartilage (Bonnevie et al., 2011; Krishnan et al., 2004; Moore and Burris, 2014), but it is often assumed to apply to both AC and hydrogels. This lack of evidence and understanding for the governing lubrication mechanisms in hydrogels limits their tribological optimisation. Therefore, we studied the fluid load support in hydrogels using a photoelastic method that provides direct evidence of the hydrogel stress distribution and thus load sharing between the solid and fluid phase. We used a reciprocating tribometer to measure hydrogel friction for several sliding conditions. To the author's knowledge, this is the first paper to use a direct experimental measure for fluid load support in a sliding contact on hydrogels. This work contributes to understanding the governing tribological mechanisms in hydrogels, which is essential to facilitate the development of better AC mimics.

1.2 Lubrication mechanisms in AC and hydrogels

Articular cartilage is a soft tissue consisting for the largest part of water (68-85%) that is contained by a matrix of mainly type II collagen fibrils (Mow et al., 2005). The cartilage structure is divided into three regions: the superficial region with fibrils arranged parallel to the surface, the middle region where fibrils are arranged more randomly in the transition from the superficial to the deep region, and the deep region where the cartilage connects to the bone and fibrils are arranged perpendicular to the bone (Mow et al., 2005). Because of the arrangement of the fibrils, cartilage has a high tensile stiffness in the direction of the fibrils compared to its compressive stiffness. The natural lubricant in human joints is synovial fluid, which is a dialysate of blood plasma and contains multiple proteins, lipids, and hyaluronic acid (Ateshian and Mow, 2005). Although there have been many papers (for example (Caligaris and Ateshian, 2008; McCutchen, 1962; Moore and Burris, 2017)) in the last sixty years analysing AC lubrication, no unifying theory has been established. Both the composition of synovial fluid and the structure of the AC matrix play an important role in the lubrication of AC, and lubrication theories can be divided into two general types:

a. Biphasic lubrication: the biphasic cartilage matrix plays an active role in film formation and load support. Examples are the weeping lubrication (McCutchen, 1962, 1959), boosted lubrication (Walker et al., 1968), fluid load support (Ateshian et al., 1998; Caligaris and Ateshian, 2008), and tribological rehydration (Moore and Burris, 2017).
b. Boundary film formation: formation of a low-shear strength film of molecules adsorbed at the cartilage surface (Jahn et al., 2016).

We will further elaborate on the biphasic lubrication mechanisms, and particularly on fluid load support, because this theory is often associated with the tribological behaviour of hydrogels as well (Baykal et al., 2013; Murakami et al., 2014; Parkes et al., 2015).

Biphasic lubrication theories describe the role of the interstitial fluid in the lubrication of AC. Generally, when a poroelastic material is deformed, the interstitial fluid may be pressurised and will resist the deformation of the material until the fluid flows away from the deformed area and insufficient pressure remains to resist deformation. One of the firstly proposed biphasic lubrication theories is the 'weeping' lubrication mechanism (McCutchen, 1962, 1959), where the interstitial fluid is thought to weep out of the matrix and form a lubricating layer on the articulating surface. The fluid load support theory (Ateshian et al., 1998) builds on this by arguing that when the interstitial fluid is pressurised, there is a load distribution over the fluid and solid phase at the contact interface without fluid squeeze out. This resulted in a model that predicts that the friction coefficient is directly related to the fraction of load carried by the fluid. When this fraction diminishes to zero, an equilibrium friction state is reached, as observed in several studies into the friction of cartilage (Accardi et al., 2011; Caligaris and Ateshian, 2008). Another early theory is the 'boosted' lubrication that suggests that water from the synovial fluid will flow into the cartilage matrix during sliding, resulting in a highly viscous and concentrated synovial fluid as lubricant on the AC surface (Walker et al., 1968). Recent studies, both numerical (Accardi et al., 2011) and experimental (Moore and Burris, 2017) support the idea that fluid flows into the cartilage in the contact area. Moore and Burris (Moore and Burris, 2017) argue with their 'tribological rehydration' theory that it is the pressurised fluid in the inlet of the contact that flows into the cartilage that provides AC with load support. The current study focussed on fluid load support as this is the main theory that is commonly related to hydrogel friction and lubrication (Baykal et al., 2013; Murakami et al., 2014; Parkes et al., 2015).

Hydrogels have similar structural properties to cartilage with a biphasic porous structure, and biphasic lubrication mechanisms are therefore often assumed to be applicable to both materials. However, the anisotropic behaviour of AC due to the orientation of the fibrils in the superficial zone is thought to be essential for the very high fluid load support in AC (Park et al., 2003). This directionality is lacking in most hydrogels, which should result in lower fluid load support. Although alternative theories exist for hydrogel lubrication (Dunn et al., 2014; Pitenis et al., 2014), biphasic theory including fluid load support is used for hydrogels as the basis for numerical studies (Baykal et al., 2013; Murakami et al., 2014) and fluid load support is used as explanation for the frictional behaviour in experimental work (Baykal et al., 2013; Milner et al., 2018). An increase of the friction coefficient over time is often seen as an indication for the presence and subsequent loss of fluid load support (Li et al., 2010; Murakami et al., 2014; Parkes et al., 2015), but friction measurements alone do not provide direct evidence for the load support mechanism.

Direct evidence is required in order to distinguish between contributions of lubrication mechanism that may occur simultaneously, such as hydrodynamic film lubrication. Primary information for direct evidence could for example be the fluid pressure or solid stress in the biphasic material. Because fluid load support is associated with the frictional behaviour of hydrogels without supporting direct evidence, we developed a photoelastic method that provides a measure for the solid stress in the hydrogel. Measurements of fluid pressure have been used before on AC (Krishnan et al., 2004), but this method limits measurements to the face opposed the interacting AC surface and does not account for spatial variations in the material. Another method, that is related to measuring the solid stress in the matrix, uses the indentation depth as a measure for fluid load fraction (Bonnevie et al., 2011; Moore and Burris, 2014). The developed photoelastic method in the current study is considered a more appropriate method to use in the presented tribological tests of hydrogels, as it allows measurement of the stress distribution throughout the entire sample. In addition, the photoelasticity method does not require an initial contact criterion to establish the zero-displacement baseline and omits the use of high-accuracy displacement measurements.

Most of the evidence for the fluid load support theory has been derived indirectly from friction measurements (Caligaris and Ateshian, 2008; Parkes et al., 2015). The measured friction depends on the test conditions and configuration of the test. Various test configurations have been used where AC is rubbed against an artificial counter face under simulated physiological conditions. The two most common contact configurations are schematically shown in Figure 1. Depending on the specimen configuration used, AC will give low sustainable friction coefficients (~0.02-0.03) over an extended test period (Caligaris and Ateshian, 2008; Moore and Burris, 2017). This can be achieved by using a 'migrating contact area' (MCA) setup where the counterface moves across the AC surface and allows fluid replenishment of the out-of-contact zone (Caligaris and Ateshian, 2008). However, if the test configuration is such that there exists a 'stationary contact area' (SCA) on the AC surface, the friction tends to increase with rubbing time reaching an equilibrium value as observed in several studies (Accardi et al., 2011; Caligaris and Ateshian, 2008). The presented explanation is that fluid exudes from the contact because of the continuously loaded area, which results in a loss of fluid load support. In a recent paper Moore and Burris (2017) challenge this relationship between a SCA and fluid load support and argue that hydrodynamic pressure drives the interstitial fluid flow, as they are able to sustain low friction in SCA using a convergent cartilage sample and relatively high sliding velocities. So far, little attention has been paid to the different configurations that can be used to achieve a continuously loaded contact: by using a convergent (cSCA) cartilage or hydrogel sample on a flat counter face (Moore and Burris, 2017), by using a stroke length that is smaller than the contact diameter (Accardi et al., 2011), or a combination of both (Caligaris and Ateshian, 2008). We use both the friction measurements and the photoelastic data to argue that the experimental configuration needs more attention, as will be discussed in section 4.3.

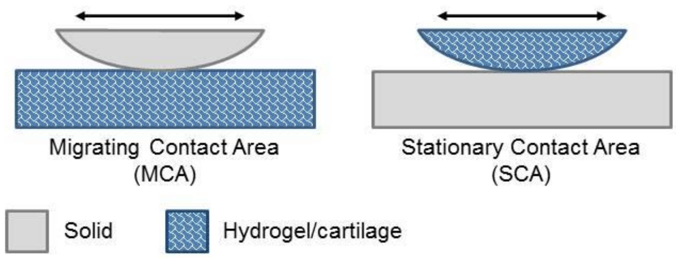

Figure 1: Schematic of contact configurations of a migrating and stationary contact area

The foregoing review has summarised the current theories of the fluid load support in AC and hydrogels. However, at present, direct experimental evidence supporting this mechanism is lacking and observations are highly dependent on the sample test configurations (MCA/SCA) used. It is important to investigate the fluid load support of hydrogels in greater detail, since friction is an essential determinant in the performance of articulating surfaces like cartilage. In addition, a thorough understanding of the friction and lubrication will help design materials that are optimized for in-contact shear conditions. To achieve this we have developed a combined friction and photoelastic test for hydrogels, which will provide measurements of the stress response of the material under loading and shear (sliding).

1.3 Aims and Method

The aim of this study was to provide direct evidence for load sharing between the solid and fluid phases in hydrogels by developing and using photoelastic method. Photoelasticity is an imaging technique that uses the birefringence of materials to determine their stress state. The stress in photoelastic materials shows as a colourful fringe pattern when exposed to polarised light. In general, the more fringes appear, the higher the stress in the material. As an example, Figure 2 shows the photoelastic fringe pattern of a Hertzian line contact in a hydrogel.

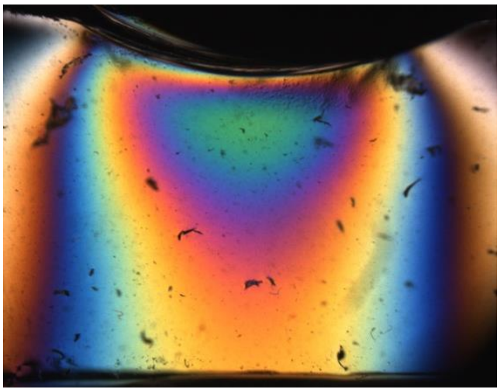

Figure 2: Photoelastic pattern showing Hertzian contact in hydrogel

Photoelasticity is well known in the field of solid mechanics (Kuske and Robertson, 1974; Shukla and Dally, 2014) and has proven very useful to study the stress in complex structures before numerical modelling became widespread. The method has also been used in biomechanics and biomaterials to study, for example, knee prostheses (Murakami et al., 1993), dental implants (da Costa Valente et al., 2017; Goiato et al., 2017) and needle insertions (Tomlinson and Taylor, 2015). The method is also used for studying the contact mechanics of granular materials (Daniels et al., 2017; Majmudar and Behringer, 2005) but has not been recently applied in the field of tribology.

Photoelasticity is a useful tool to directly investigate the load sharing in the hydrogel, because the stress in the solid matrix will be affected by the ratio of the load sharing between the fluid and solid phase of the hydrogel (Murakami et al., 2015). In poroelastic materials the deformation of the solid matrix will be lower in a fully hydrated state compared to a drained state, because of the fluid component carrying part of the load. The lower strains consequently result in lower stress in the solid matrix. Any change in fluid load support will lead to changes in solid stress, and should therefore be observable as a change in the photoelastic response.

Photoelastic hydrogels have been used before by Tomlinson and Taylor (Tomlinson and Taylor, 2015), who explore the photoelastic use of konjac, gelatin and agar gels. In this study we chose to develop a photoelastic poly(vinyl alcohol) (PVA) hydrogel, because of its higher stiffness and the common use of PVA as cartilage mimic (Spiller et al., 2011). The photoelastic technique was used to visualise the stress field in the solid matrix of the hydrogel during sliding tests. Using photoelasticity in tribological measurements of hydrogels is a new approach to provide a direct measure for fluid load support in sliding conditions.

2. Materials & Methods

2.1 Photoelasticity

Figure 3 shows a typical photoelastic setup, comprising a light source and two (circular) polarisers. The light from the light source is polarised by the first polariser before reaching the object. Because of the birefringence of the object, in this study a PVA hydrogel sample, the refraction of light depends on the direction and magnitude of the principal stresses σ_1 and σ_2 (Shukla and Dally, 2014), as illustrated in Figure 3. The difference in refraction results in a phase shift when the light exits the material, as visualised in the inset in Figure 3. After polarisation by the second polariser, called the analyser, the directionality is removed and the phase shift is the only difference between the waves. The phase difference Δ can be expressed as:

$$\Delta = \frac{2\pi hc}{\lambda}(\sigma_1 - \sigma_2) \tag{1}$$

with h the thickness of the material, c the relative stress-optic coefficient of the material, λ the wavelength of the light and σ_1 and σ_2 the principal stresses in the material in plane stress.

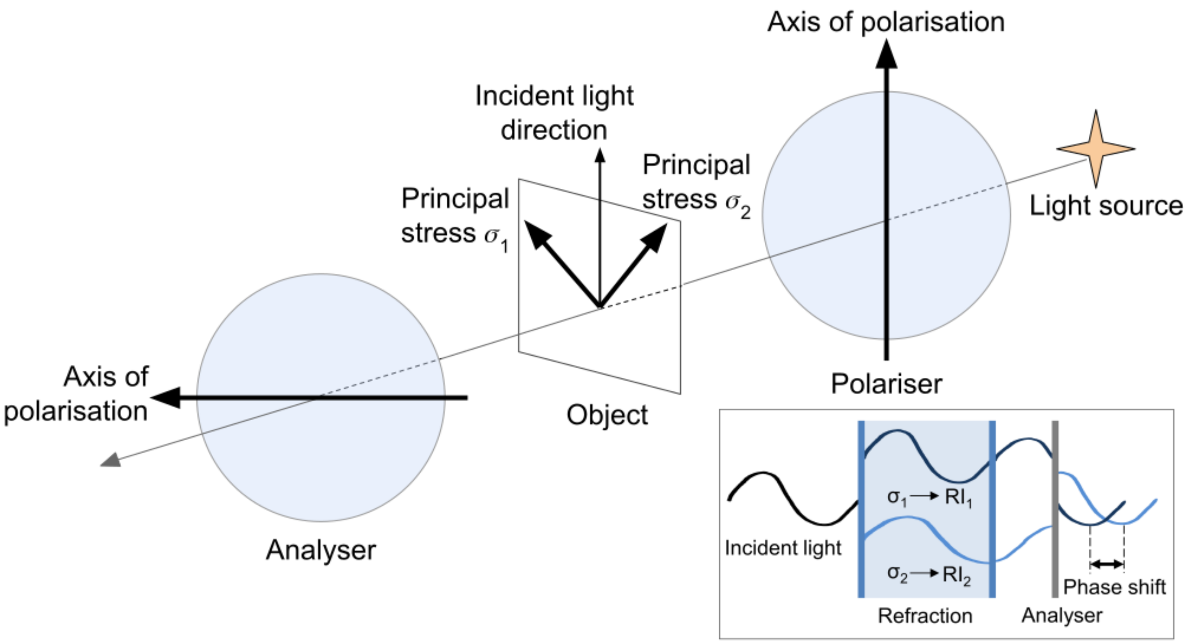

Figure 3: Schematic of photoelastic setup and, inset, a simplified visualisation of birefringence and the resulting phase shift

For each non-zero value of (σ_1- σ_2) a specific wavelength is extinguished from the light (Shukla and Dally, 2014). This results in the typical fringe pattern observed in photoelastic materials, as was shown in Figure 2. Monochromatic light can be used to simplify the analysis, as the colourful pattern reduces to a black and white fringe pattern. In this study a blue light filter was used in the experiments, which resulted in a pattern of black and blue fringes that could be easily modified to a greyscale image for analysis. The order of extinction, visible as the number of fringes n, can be expressed as:

$$n = \frac{\Delta}{2\pi} = \frac{hc}{\lambda}(\sigma_1 - \sigma_2) \tag{2}$$

The relationship between the number of fringes and the stress state is material specific and determined by the 'relative stress-optic coefficient' c. Fringe patterns can therefore only be compared between samples with the same stress-optic coefficient, and the stress-optic coefficient will have to be obtained to enable quantitative measures.

Figure 4 shows the photoelastic response of a PVA hydrogel sample under static loading between 0-2 N with a cylindrical lens. The images show a clear distinction between the stress states under different loading conditions. When no load is applied the image is almost completely black with only a small residual stress from the manufacturing process (Figure 4a). For a small load of 0.5 N a single fringe appears in the material (Figure 4b), showing a stress distribution conforming to Hertzian contact theory. The number of fringes increases for increasing load and a second black fringe appears in the image with the highest load (Figure 4e), whereas only a single black fringe is seen in the other images.

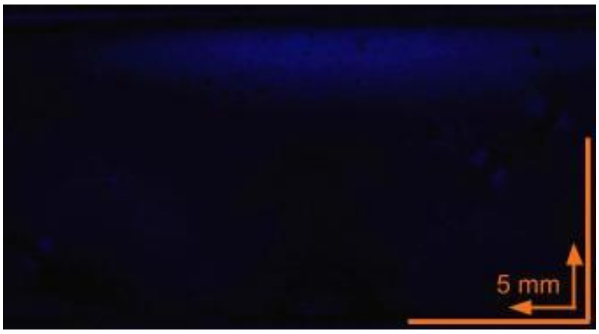

(a) 0 N

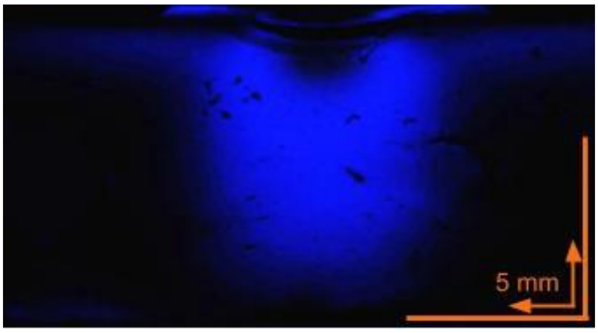

(b) 0.5 N

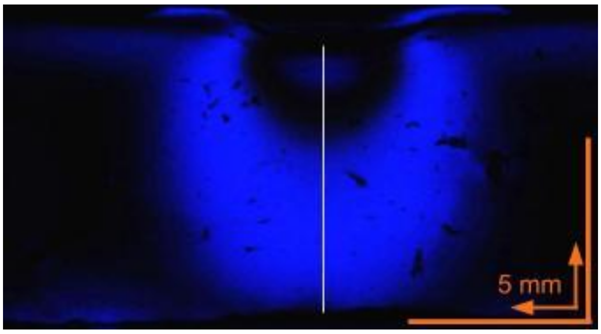

(c) 1.0 N

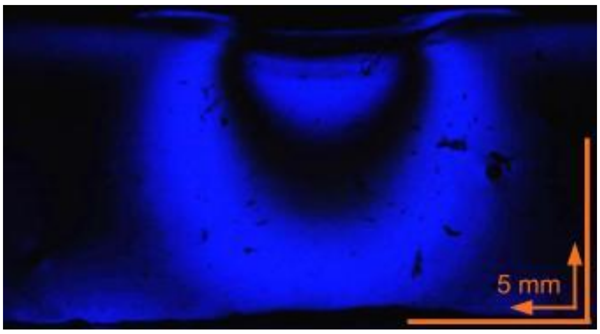

(d) 1.5 N

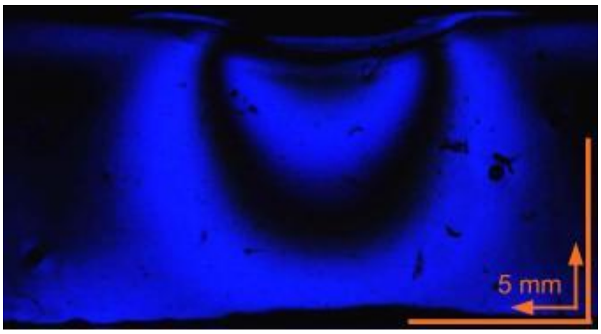

(e) 2.0 N

Figure 4: Photoelastic images of static loading with (a) no load, (b) 0.5 N load, (c) 1.0 N load, (d), 1.5 N load, and (e) 2.0 N load

Intensity profiles taken through the centre of the contact can be helpful to analyse smaller changes in the load. The white line in Figure 4c shows the segment along which the intensity profiles are taken. This segment is identical for each analysis. Figure 5 shows two intensity profiles, comparing the 1 N and 1.5 N images (Figure 4c and 4d). The intensity on the x-axis is normalised to the highest peak in the measurements and the y-axis represents the depth into the hydrogel from the surface. The number of fringes can be read from the number of peaks in the graph, which is two in both cases. The stress change can be observed from two other features in the intensity graphs. The 1.5 N profile shows a clearly higher intensity for the second fringe and a shift downwards along the profile, which is most clearly visible for the first fringe. Both the images and the intensity profiles are used in this research to perform photoelastic analysis.

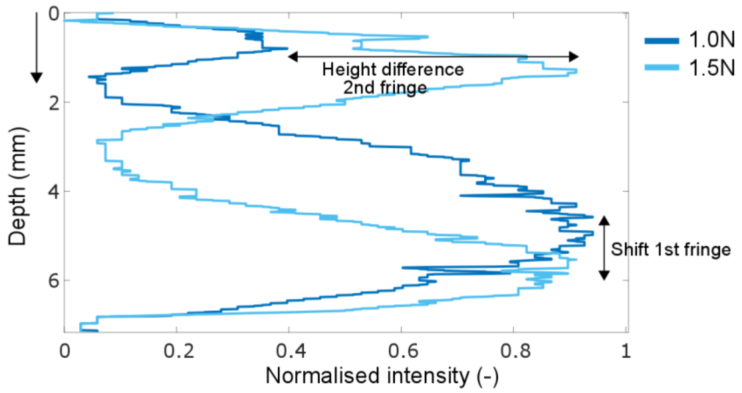

Figure 5: Intensity profiles comparing 1.0N and 1.5N load

Although the stress-optic coefficient is not determined for the hydrogels, the intensity profiles can be used to obtain an estimate for the relationship between the load and fringes. The profiles in Figure 5 show that in case of a 1.0 N load about 1.4 fringes appear and in case of a 1.5 N load about 2 full fringes are visible. On average, when also taking into account the profiles not shown in Figure 5, the fringe pattern changes with about one full fringe per N load. Based on the assumption that the material will not show fluid load support in case of static loading, the full load will be carried by the solid: $F = F_s$. If there is any fluid load support in a sliding contact, the applied load in that case will be carried by both the solid and the fluid: $F = F_s+F_{FL}$. Comparing the number of fringes from the sliding contact to a static contact load will give an estimate of the magnitude of the load carried by the fluid (F_{FL}), because the applied load (F) is known and the load carried by the solid matrix (F_s) can be estimated from the photoelastic images.

2.2 BioTribometer

The BioTribometer ((BTM), PCS Instruments, UK) is used to perform friction tests during which the photoelastic response of the hydrogel was recorded. Figure 6 shows a schematic of the BTM integrated with the photoelastic setup. The top specimen was a 12.5x20 mm glass PCX cylinder lens with a radius of 9.81 mm (#68-029, Edmund Optics, UK) and the bottom specimen was a rectangular hydrogel sample (±45x8x8 mm) that will be further specified in the next section. The glass lens was brought into a reciprocating sliding contact with the hydrogel sample with specified load, stroke length and frequency. The contact was lubricated with a thin film of 30 µl ultra-pure water on the surface of the hydrogel. A test was also run on a sample without adding lubricant to study the self-lubricating ability of the hydrogel. The top specimen can be independently actuated in three directions using brushless motors. Friction forces were measured by two force transducers in the bottom platform. The applied load was measured with a third force transducer connected to the reciprocating glass lens. The BTM was specifically designed to mimic physiological conditions with a load range of 0.5-5 N and a reciprocating frequency range of 0.1-5 Hz. All data was recorded continuously and synchronised using NI data acquisition and is directly available in LabView. The photoelastic response of the hydrogel is captured by a camera (Grasshopper 3, Point Grey Research, Canada) and analysed using Matlab.

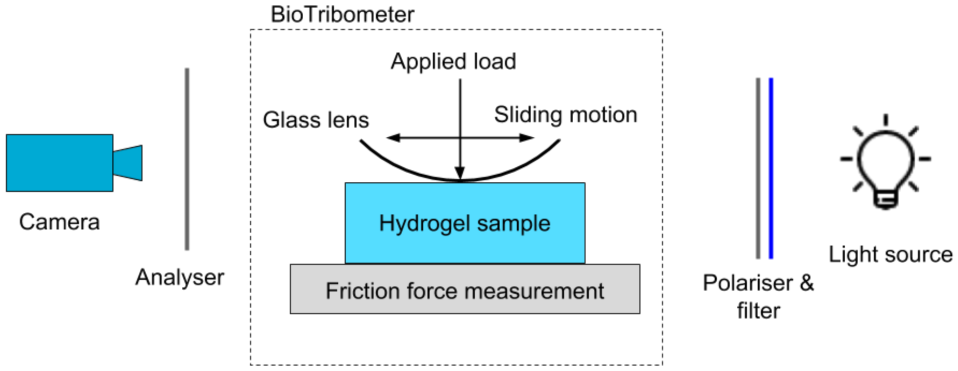

Figure 6: Schematic of the BTM and photoelastic setup

Tests are performed using two different sliding conditions, as indicated in Table 1. Both continuously and intermittently loaded areas are present in a joint during a full gait cycle (Wang et al., 2017), and therefore stroke lengths of 3 mm and 7 mm are chosen to represent this physiological condition: part of the contact will be continuously loaded for a 3 mm stroke length and be migrating for a 7 mm stroke length. The graphic summary in the table illustrates these different contact configurations. Each test condition is performed twice on three different samples. The contact width is estimated to be 5 mm from the photoelastic images taken during the tests. The samples have a width between 6-7 mm, which resulted in an approximate contact pressure of 0.03 MPa. The friction coefficient is calculated by taking an average value over the middle 50% of each stroke to discard the effect of the turning point.

Table 1: Test conditions for the 'short stroke' and 'long stroke' configuration

Test conditions	General	
Applied load	1 N	
Sliding velocity	20 mm/s	
Approx. contact width (2a)	≈ 5 mm	
Approx. contact pressure	≈ 0.03 MPa	
	Short stroke	**Long stroke**
Stroke length	3 mm	7 mm
Frequency	3.33 Hz	1.43 Hz
Graphic summary of the contact conditions	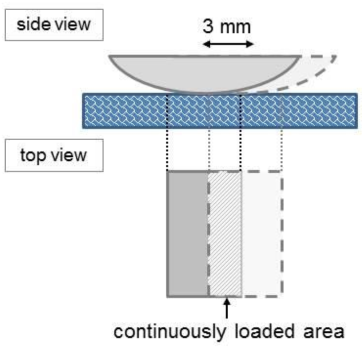	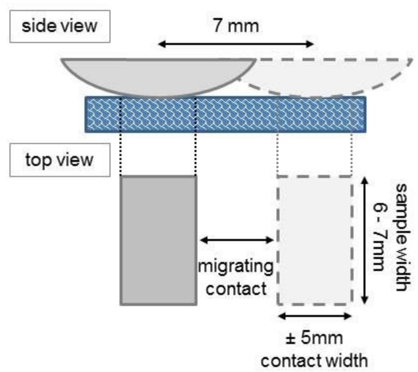

2.3 PVA hydrogels

In order to use the photoelastic technique for hydrogels, it is essential to have a transparent material. The commonly used freeze-thaw method for PVA hydrogels (for example (Holloway et al., 2013) is unsuitable as this results in an opaque material (Peppas, 1975). To produce transparent PVA hydrogels, the method described by Hyon et al. (1989) was used. Adding di-methyl sulfoxide (DMSO) to the solvent gives a finer and more regular pore structure to the hydrogel (Hou 2015, Hyon 1989), which results in high light transmittance. For optimal light transmittance, 15%w PVA pellets (Mw 146,000-186,000, 99+% hydrolysed, Sigma Aldrich, UK) were dissolved in a mixture of 80%w DMSO (≥99%, FG, Sigma-Aldrich, UK) and 20%w ultra-pure water. The mixture was initially heated and stirred on a magnetic hotplate at 135˚C for about 20-30 minutes to create a homogenous solution. The solution should be transparent and homogenous, but individual pellets may still be visible. At this stage, the solution was too viscous to be stirred on the hotplate and was transferred to a pressure cooker (CuisinArt) to evenly heat the mixture at elevated temperatures. After 20 minutes of pressure cooking the mixture was stirred manually to maintain a homogenous solution. This heating and subsequent stirring was repeated three times, without stirring the mixture after the last repeat to avoid entrapping additional air in the mixture. Any remaining subsurface bubbles were removed with a vacuum pump or in an ultrasonic bath. Hydrogels were moulded in two shapes; a ø21x8 mm cylinder and a 45x120x8 mm rectangle. Cylinder moulds were filled with 2.5-3.0 ml each and rectangular moulds with 43 ml, resulting in a height of about 8 mm for both moulds. The mixture was subsequently reheated in the pressure cooker to remove shear stress induced by the moulding process. The PVA gels were then frozen for 20h at -23˚C. After removing the gels from the freezer, the two ends of the rectangle were cut at 8 mm from the edge to create samples of 45x8x8 mm with three smooth surfaces. All samples were stored in ultra-pure water, which was regularly changed for at least a week to rinse the DMSO from the samples. The samples shrink about 1-2 mm during the rinsing process, resulting in varying width and thickness between 6-8mm. The final water content of gels made with this procedure was typically 74 w%. The cylindrical samples were used for compression and indentations tests and the rectangular samples were used for friction tests.

2.4 Material characterisation

The Mach-I™ (Biomomentum, Canada) was used to perform stress-relaxation tests to determine the maximum fraction of fluid load support. The pre-programmed stress relaxation function of the machine was used to determine the poroelastic behaviour of the material for different strain rates. Cylindrical hydrogel samples of ø20 mm and 6-8 mm thick are compressed using a flat aluminium indenter with a larger radius (ø40 mm) to ensure even compression across the sample. The thickness of the samples was measured by recording the z-position of the indenter while applying a small load of 0.1 N to ensure contact with the sample. Samples were compressed to about 15% strain with velocities ranging from 0.5 to 20mm/s. The relaxation of the material is measured for 300s as this is the same duration as the friction tests.

To measure the elastic modulus of the material, cylindrical hydrogel samples with the same dimensions (ø20 mm and 6-8 mm thick) are compressed using the same setup up to a force of 1.5 N at 0.5mm/s. The resulting stress-strain curves were fitted with a 2nd order polynomial, as shown by the example in Figure 7a. From the fitted curves the elastic modulus is determined and given in Figure 7b. The hydrogels have a strain dependent modulus ranging from about 0.1-0.25 MPa.

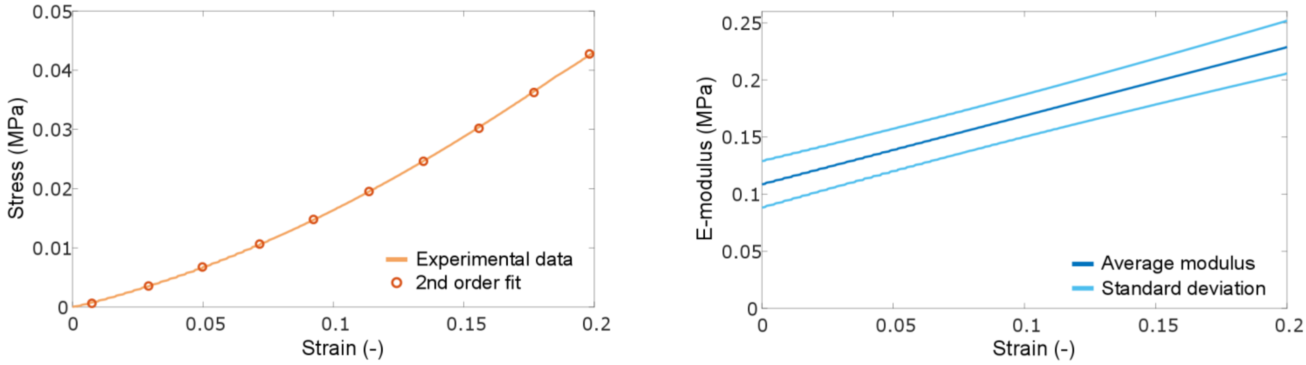

(a) Curve-fitted result (b) Elastic modulus from curve-fitted results (n=6)

Figure 7: Material characterisation based on compression tests with the Mach-I^{TM}

3. Results

3.1 Friction

Friction tests were performed on the BTM with 3 mm and 7 mm stroke lengths, as previously shown in Table 1, resulting in a continuously loaded area (stroke length < 2a) and a MCA condition (stroke length > 2a), respectively. Figure 8 shows the friction coefficient over time for these two conditions, with the dark line showing the average value and the light coloured lines indicating the standard deviation. For the 7 mm stroke length a low friction ($\mu \approx 0.02$) is maintained over the entire duration of the test whilst for the 3 mm stroke length the friction coefficient increases over time, approaching an equilibrium of about μ = 0.4-0.5 at the end of the test. The low friction value observed under MCA conditions is thus less than 5% of the high equilibrium value. A test without any externally applied lubricant resulted in much higher friction ($\mu > 0.7$). Similar friction results to those shown in Figure 8 have been reported in studies on AC (Caligaris and Ateshian, 2008), but the clear distinction in friction between the MCA and continuously loaded conditions has not been directly reported before in studies on hydrogels. Any differences between the stable low friction and the high equilibrium friction regimes are usually thought to be caused by the loss of fluid load support in the latter case (Caligaris and Ateshian, 2008). Photoelastic images taken during the friction tests provide insight into the fluid load support of the hydrogels.

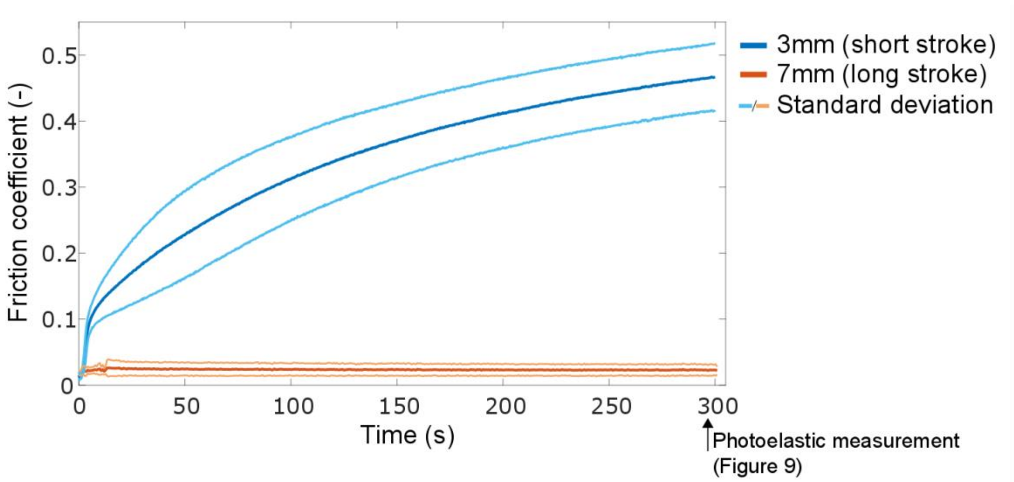

Figure 8: Average friction coefficient over time for 3 mm and 7 mm stroke length (n=6)

3.2 Photoelasticity and the subsurface stress field

Photoelastic images from tests with long and short stroke lengths are compared to each other to establish the contribution of fluid load support to the frictional behaviour. Figure 9 shows images taken with a static normal loading (Fig 9a, repeated from Fig 4), in the low friction regime with a 7 mm stroke length (Fig 9b), and when the high equilibrium friction has been reached with a 3 mm stroke length (Fig 9c). The images were taken just before the end of the test, as indicated by the arrow in Figure 8. All images show a very similar fringe pattern and the photoelastic images taken during friction tests do not deviate significantly from the static loading condition. If the different sliding conditions would result in any major changes to the fluid load support, the stress in the hydrogel during sliding with the long stroke length and low friction (Fig 9b) should clearly show a reduced solid stress (Murakami et al., 2015). Another observation that can be made directly from the image for high friction during the short stroke test (Fig 9c), is that a shear component is visible as a skewed fringe pattern in the direction of sliding. This is due to the contribution of the friction force, which changes the direction of the resultant force on the hydrogel, as indicated by the arrow in Figure 9c.

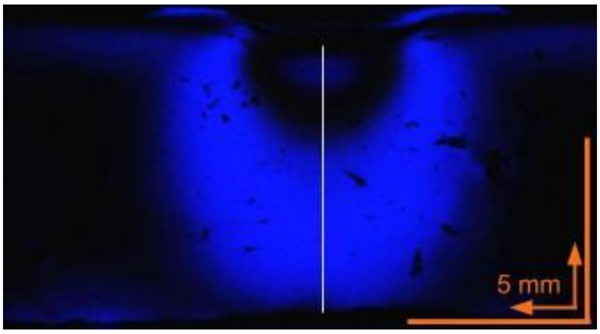

(a) 1.0 N – static loading - white line indicates intensity profile measurement

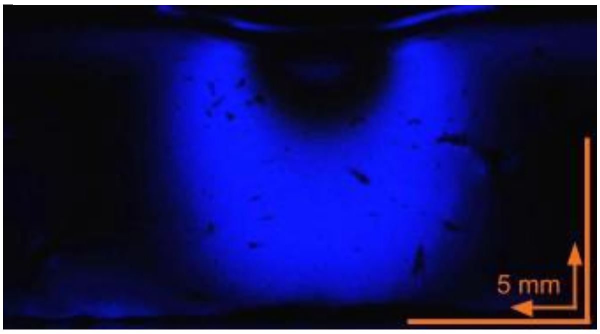

(b) 1.0 N – long stroke, low friction

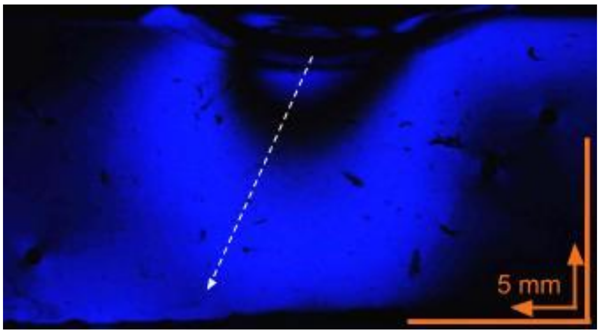

(c) 1.0 N – short stroke, high friction – white arrow indicates direction of resultant force

Figure 9: Photoelastic images taken at (a) static loading, and during sliding tests with (b) long stroke length (i.e. low friction), and (c) short stroke length (i.e. high friction).

A more detailed comparison can be made using the intensity profiles through the centre of the photoelastic images, as shown in Figure 10. The observed change in the peak height of the second fringe and the shift along the profile of the first fringe indicate minor changes in the stress. For sliding with a long stroke length the stress is somewhat reduced compared to static loading, whilst for the short stroke length a slightly increased stress is observed compared to static loading. Using the relationship of 1 N/fringe the load for the 3 mm and 7 mm stroke were estimated at about 1.1 N and 0.9 N respectively. This higher load can be attributed to the increased friction component, for a friction force of about 0.45 N the resultant force acting on the hydrogel is about 1.1N. The reduced load for the 7mm stroke is however not observed in all samples and would also only mean a small contribution of about 10% fluid load support. This potential contribution would not be enough to explain the observed frictional behaviour of the hydrogels.

The photoelastic results did not show the hypothesized relationship between the stress field and the friction of the hydrogels. If the friction difference is driven by a change in the fluid load support, then the images and intensity profiles from tests with short stroke length and high friction should show a major increase of the stresses in the hydrogel. To obtain additional evidence for the lack of fluid load support in the hydrogels, a number of stress-relaxation tests were performed on the specimens.

3.3 Stress relaxation

Stress relaxation tests provide insight into fluid load support because the interstitial fluid in the hydrogel specimens will be pressurised during the initial loading phase and subsequently lose pressure over time. Although the solid matrix may show some viscoelastic behaviour itself, the difference between the peak stress and the stress after relaxation could be used as a measure for maximum fluid load support. Therefore, stress relaxation tests are performed with different compression rates ranging from 0.5-20mm/s. Figure 11 shows the difference between the peak force and relaxation force after 300s for four different rates. The relaxation percentage is highest for the highest compression rate, but only by a few percent compared to the lowest rate. Since the maximum relaxation percentage is not more than 15%, it is expected that the maximum fluid load support can only change with a maximum of 15% of the total load as well. Although the effect on the friction coefficient is also dependent on the solid-to-solid fraction and the initial fluid load fraction (Ateshian, 2009), a 15% reduction of the fluid load support will not result in the 95% difference observed in this study. These relaxation results support the photoelastic results as they indicate only a limited change in fluid load support over the same duration as the friction tests.

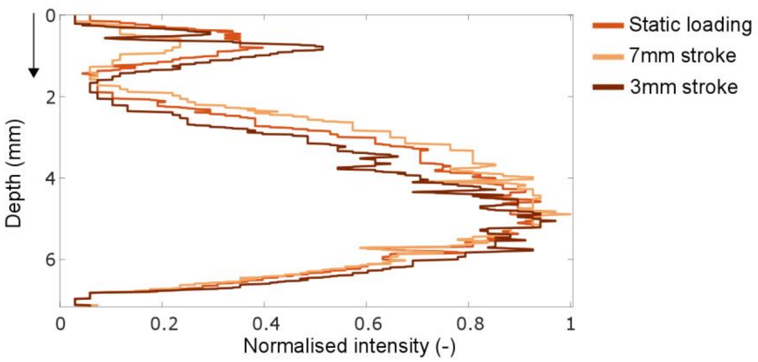

Figure 10: Intensity profiles (from images Figure 9) comparing the stress of the hydrogel for different configurations

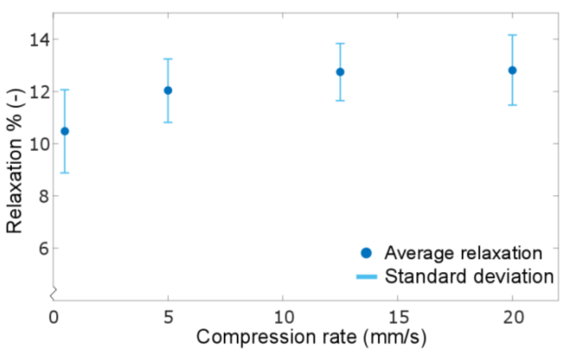

Figure 11: Average % relaxation, including standard deviation (n=4)

4. Discussion

4.1 The photoelastic measurement technique

This paper describes the use of photoelasticity for visualising the stress field in hydrogels during sliding interaction. Photoelastic methods have been employed to study stresses in soft biomaterials like gelatine (Murakami et al., 1993; Tomlinson and Taylor, 2015), but have not been used before to systematically study the frictional behaviour in biotribological tests. The successful implementation of photoelasticity in the friction experiments means that this method can be used to gain insight into the contact and friction mechanics of soft biomaterials in general and the fluid load support mechanism in PVA hydrogels in particular. The use of photoelasticity can both enhance our understanding of the behaviour of these materials and be beneficial to validate numerical models describing stresses and strains in sliding interactions.

The photoelastic method as used in this paper has several limitations. One general restriction is that materials have to be optically transparent in order to be able to record the stress response. This restricts its use as many biomaterials are non-transparent, including PVA hydrogels made with different ratios of water and DMSO as solvents (Hou et al., 2015; Hyon et al., 1989). Altering the optical properties of the hydrogel inherently means a change to the structure (Hou et al., 2015; Kita et al., 1990). The photoelastic method is however not limited to the polymer concentration of the hydrogels used in this study. Hydrogels were also prepared with very low polymer concentration (2%), and although these showed a weaker photoelastic response, fringes were still visible upon loading.

Another limitation is that the photoelasticity is currently implemented in a line contact geometry, meaning the resulting stress field is two-dimensional. Implementation in a circular contact adds complexity to the measurements because of the three dimensional stress fields. A possible way to account for the stress variations along the thickness of the sample is to combine the experiments with a computational model that simulates the spatial effects. In addition, a control measure should be used to support the photoelastic measurements, as the technique was only used to provide evidence for the lack of fluid load support. In the recent study, stress relaxation measurements provided this supporting evidence. Other measurements to study the materials' potential for fluid load support include fluid pressure measurements, and indentation frequency sweeps.

The quantification of the relationship between fringes and load that was used in this study, is only a valid estimate for the specific setup used. The relationship will only hold for samples that have been made following the same procedure, that have roughly the same thickness, and that are loaded with the same indenter. Obtaining quantitative data from the photoelastic images is possible after a calibration that relates a known stress state to the number of fringes. Usually the analytical solution to a cylinder in diametrical compression is used for calibration (Shukla and Dally, 2014). However, for materials such as hydrogels with a relatively low stiffness the analytical solutions are not valid because of the large deformations, whilst the strain dependent stiffness (Figure 7) of the hydrogels add further complexity. Therefore, the calibration equations should be solved numerically. In addition, it is very likely that the stress optic coefficient varies between samples. A quantitative analysis will therefore give an estimate of the stress in the material, based on an average value of the different stress optic coefficients.

4.2 Fluid load support in hydrogels

The photoelastic method provides direct evidence for fluid load support mechanism in hydrogels. Numerical models (Murakami et al., 2015) show that the fluid pressure and the solid stress in hydrogels are directly related, because a reduction of the fluid pressure directly leads to increased stresses in the solid. Fluid load support is commonly associated with the tribological behaviour of hydrogels (Baykal et al., 2013; Li et al., 2010; Parkes et al., 2015), and it was therefore expected that a major change in the tribological behaviour of the tested hydrogels would relate to a major change in the photoelastic stress images. Friction tests with a short stroke resulted in much higher friction coefficients than tests with a long stroke length, but the photoelastic images did not show alterations in the stress patterns that indicated major changes in fluid load support. This does not exclude the existence of a load sharing mechanism between the solid and fluid phase, but rather shows that there are only small changes within the duration of the tests. Therefore, fluid load support cannot be the main driver behind the differences in frictional behaviour observed for the hydrogels.

The photoelastic results were supported by stress relaxation experiments. For velocities and time scales comparable to those used in the friction experiments, the hydrogels showed a nearly elastic behaviour, with a maximum of 15% relaxation of the stress. This is in line with elastic behaviour observed by (Schulze et al., 2017), who argue that hydrogels behave elastic rather than poroelastic if the applied pressure does not exceed the osmotic pressure. Additional photoelastic images taken over a 300 s period of extended static loading with the cylindrical lens and 1 N load on the BTM showed that the contact area slightly increased due to the relaxation of the material, which was expected from the relaxation tests. The fringe pattern indicated a slight increase of the stress during the relaxation of the material, which could indicate a loss of fluid load support and an increase of solid stress. It should be kept in mind that many viscoelastic polymers have a time dependent stress-optic coefficient that usually results in an increasing number of fringes over time under constant loading (Shukla and Dally, 2014). Although the viscoelastic behaviour of hydrogels is reported to be primarily depended on interstitial fluid flow (Baykal et al., 2013; Stammen et al., 2001), this is challenged by Schulze et al. (2017). It is therefore not clear if the observed relaxation of the material was due to a loss of fluid load support. Nonetheless, the time scales of all tests in the current work are identical, and these results were therefore not affected by any time dependent stress-optic coefficients.

Surface damage of the hydrogel specimens was considered as a possible explanation for the distinct frictional behaviour shown in Figure 8, but repeat tests on the same sample resulted in similar friction traces. Altering the test conditions from short to long stroke lengths could be randomly repeated and tests with a long stroke length would always show a low stable friction coefficient, independent of the testing history of the used specimens. This shows that the observed high friction regime is not caused by damage to the surface, as this would have affected the further tests on the sample. In addition, visual inspection with a microscope also did not show any indication of damage to the surface. A self-lubricating mechanism by fluid exudation from the matrix (Accardi et al., 2011; McCutchen, 1962) was also not observed, as a friction test without any added lubricant resulted in very high friction on the PVA hydrogels. The observed differences in friction traces between short and long stroke lengths is therefore thought not to relate to progressive surface damage or a self-lubrication mechanism, but to relate to the external lubrication of the material.

The observed increasing friction coefficient with time has also been reported in literature, both for tests on cartilage (Accardi et al., 2011; Caligaris and Ateshian, 2008; Murakami et al., 2014; Parkes et al., 2015) and hydrogels (Dunn et al., 2014; Murakami et al., 2014; Parkes et al., 2015), but only a few (Caligaris and Ateshian, 2008; Dunn et al., 2014) include both a migrating and stationary contact configuration in their study. Dunn et al. (2014) report an increasing friction for their hydrogels in an stationary contact area (SCA) configuration, but the observed rate of increase is much lower than that found in the present study. This could relate to the different testing conditions, such as the much lower sliding velocities and applied normal load in their experiments. Additionally, it may also relate to the different experimental configuration of a hydrogel lens sliding on a flat glass surface, whereas in our study we use a glass lens against a flat hydrogel with a stroke length smaller than the contact width to achieve a constantly loaded area. Similarly, the difference between a stable low friction coefficient (Moore and Burris, 2017) and a high friction coefficient (Caligaris and Ateshian, 2008) for SCA may result from the different testing conditions: 20 mm stroke at 60 mm/s and 1 mm stroke at 1 mm/s respectively. Moore and Burris argue that the low friction is due to the hydrodynamic pressures, which relates to the sliding velocity, but the difference in stroke length may be equally important as we will discuss in the next section.

4.3 Replenishment of the contact

The obtained results showed that the as-prepared PVA hydrogels do not rely on fluid load support lubrication for their tribological behaviour. Also, when the test was run on a hydrogel specimen without an externally applied lubricant, a high friction ($\mu > 0.7$) was obtained from the start. In contrast, when an externally applied lubricant was used, low friction was obtained for the long stroke length (7 mm, > 2a), but not for the short stroke length (3 mm, < 2a) condition. This suggests the friction increase is due to lubricant starvation and lack of external fluid replenishment of the contact during reciprocation. Classically, lubricant starvation occurs when there is insufficient fluid to fill the inlet to the contact, preventing the full hydrodynamic pressure build-up to occur (Wedeven et al., 1971). As a result, an insufficient amount of lubricant is entrained in the contact to establish or maintain a lubricant film, resulting in increasing friction over time (Berthe et al., 2014). The lack of fluid replenishment may be due to very small volumes of lubricant available (Damiens et al., 2004), the properties of the lubricant (particularly important when using high viscosity oils or greases) (Cann, 1999), or the contact kinematics (Cann et al., 2004). Starved lubricant conditions commonly occur in systems where there are multiple successive contacts, high speeds, and high viscosity fluids, for example grease lubricated rolling element bearings (Cann, 1999).

In light of this lubricant starvation, the various test conditions and contact configurations of the various studies discussed in this paper could be part of the explanation for the frictional behaviour of the materials. Both a stable low friction (Moore and Burris, 2017) and an elevated equilibrium friction (Caligaris and Ateshian, 2008) have been reported for SCA conditions. The main driver for the interstitial fluid flow mechanism proposed by Moore and Burris (2017) is the build-up of hydrodynamic pressure in the converging inlet, with low friction observed for a convergent stationary contact (cSCA). The reduction in fluid load support and the resulting increased friction observed by Moore and Burris (2017) when a converging inlet is not present can be considered as a starved lubrication mechanism. In the current work it is the motion of the contact and the way in which it controls external fluid replenishment that is important in determining pressure build-up in the contact region.

Figure 12 shows a schematic overview of the different MCA and (convergent) SCA configurations that can be used for the tribological testing of hydrogels and cartilage. The SCA configuration with two flat surfaces is shown for completeness but will not be discussed further, as the configuration was not part of this study. In most studies (Caligaris and Ateshian, 2008; Dunn et al., 2014; Moore and Burris, 2017) a continuously loaded area is configured by using a flat rigid surface in contact with a convex hydrogel or cartilage counter surface (cSCA). In our study the contact was formed using a flat hydrogel with a cylindrical glass counter face (MCA), which resulted in a continuously loaded part of the contact only when the stroke length is equal to, or smaller than the contact width (2a). As we will argue in more detail in the following paragraphs, the short stroke length likely resulted in insufficient replenishment of the fluid film, which we will therefore call a 'non-replenished' state.

Different operating conditions lead to a range of lubrication mechanisms governing the frictional behaviour. Caligaris and Ateshian (2008) introduce the SCA and its effect on friction by changing the configuration of the cartilage and glass samples. However, they simultaneously change the length of the translation without specifically accounting for this change. Using the described configurations in Figure 12, we observed that by the simultaneous change of sample configuration and stroke length, they not only changed the configuration from MCA to cSCA, but also changed from a replenished to a non-replenished state. Similarly, Accardi et al. (2011) show a dependency of the friction coefficient on the sliding velocity by varying the stroke length to enable the velocity change. As a consequence they also change from a replenished MCA to a non-replenished MCA. In both these studies an increasing friction coefficient was observed when experiments were performed in a non-replenished state, similar to the results presented in this paper.

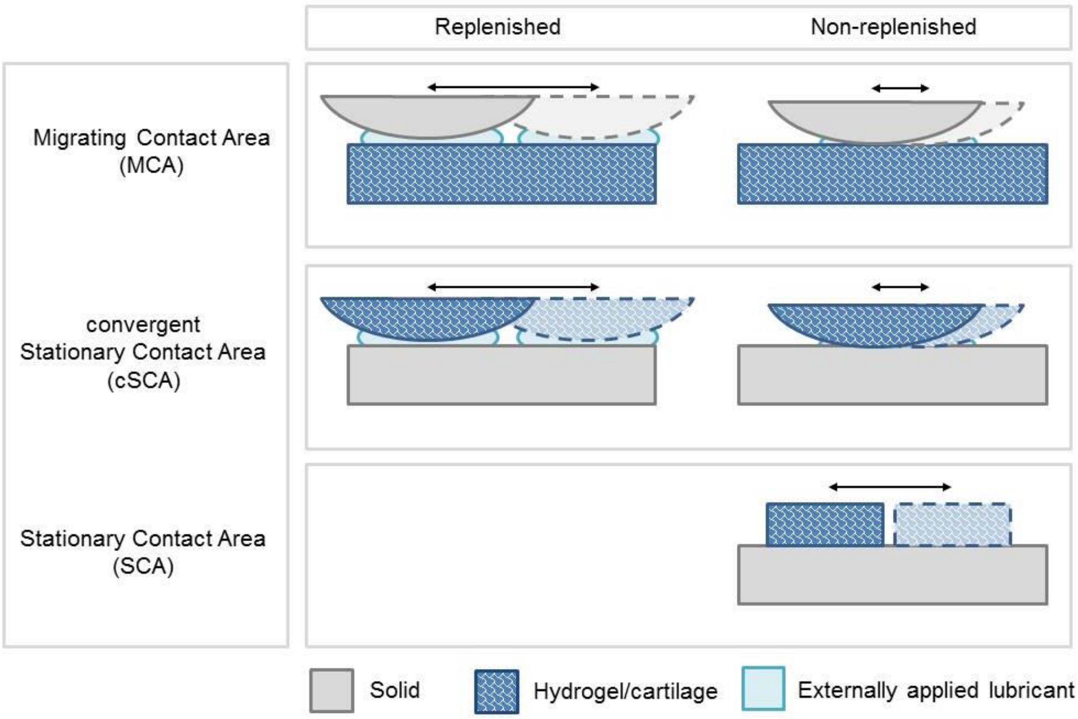

Figure 12: Different configurations of experimental contact conditions

Classical lubrication theories (elastohydrodynamic/hydrodynamic) are based on the assumption of a sufficient supply of lubricant to the rubbing contact to generate a fluid film and do not accurately describe the behaviour observed in this study. Also lubrication theories specifically established for hydrogel- or cartilage lubrication, such as hydration lubrication (Jahn et al., 2016), and polymer fluctuation lubrication (Pitenis et al., 2014), do not take into account the lubricant supply based on a change in stroke length. Fluid load support theory does account for the change in stroke length to some extent, as it suggests that if the moving contact does not have sufficient time for interstitial rehydration between loading cycles, it loses the ability to provide fluid load support. However, we show that fluid load support is not the main driver for the tribological behaviour of the hydrogels, and lubricant starvation for contacts with a relatively short stroke length (Kaneta et al., 2000; Stewart et al., 1997) should therefore be considered. The proposed non-replenished contact hypothesis should exist in parallel with the aforementioned theories that describe the lubrication for replenished contacts. Because of the contact conditions in the current study, a ‘non-replenished’ lubrication mechanism seems the most appropriate lubrication theory explaining the high friction observed in our experiments, and this mechanism will be the topic of further research.

4.4 Limitations and further research

This study focussed on the fundamental mechanisms involved in the frictional behaviour of hydrogels. It investigated the contribution of fluid load support and therefore included two test conditions that showed a clear difference in frictional behaviour and that were hypothesized to relate to a change in fluid load support. Other test conditions, such as alternative configurations, stroke lengths, and/or sliding velocities were not considered in this study, and as a result this study does not cover every situation in which high friction has been reported (Murakami et al., 2014). Changing the sliding velocity is not expected to have a big impact on the fluid load support contribution, as the relaxation behaviour of the hydrogels did not show a strong dependence on the rate of loading. Changing the motion conditions could have an effect on the hypothesized replenishment mechanism and should be considered in further research. As yet, the exact stroke length and motion frequency at which the system transitions from a replenished to a non-replenished state has not been identified, but the starved lubrication mechanism is hypothesized to apply to all stroke lengths with a smaller stroke length than the transition point. Because of the relatively large contact areas that occur for cartilage and hydrogels, lubricant starvation is an important consideration in both their application and their test conditions.

Hydrogels can be made with a range of different properties, including chemical composition, stiffness, pore size and porosity. The experimental results presented in the current study were obtained on one type of hydrogel and any possible variations of the material were not taken into account. Nonetheless, the findings of this study are highly relevant for hydrogels and cartilage in general because they show that, fluid load support cannot be assumed to be the governing lubrication mechanism from friction measurements alone. The developed photoelastic method can be used to further explore the mechanism of fluid load support for hydrogels with different physical and mechanical properties.

5. Conclusion

We studied the friction behaviour of PVA hydrogels, because hydrogels are proposed as suitable materials both for the repair of damaged articular cartilage, and as a mimic material that enables an investigation of the fundamental contact behaviour of articular cartilage. However, the poor tribological performance of hydrogels is well documented and gaining a better understanding of the tribology of hydrogels can provide useful insights for the improvement of their performance. The presented research contributes to our understanding of the tribology of hydrogels by developing a direct measure for the mechanism of fluid load support, showing that fluid load support is not necessarily the main determinant in the frictional behaviour, and emphasizing the relevance of experimental conditions.

From this study we conclude that:

- Photoelasticity is a promising method to gain more insight into the frictional behaviour of soft tissue mimics such as hydrogels. We successfully developed a photoelastic method for PVA hydrogels, which directly measures fluid load support by assessing the stress field in the solid matrix during sliding contact.
- The mechanism of fluid load support was not the main driver behind the frictional behaviour of the tested hydrogels. The observed stress fields in the hydrogels under different

conditions did not show the clear distinction necessary to be able to attribute the frictional differences to variations in fluid load support. We hypothesized that the replenishment of the lubricant may be a more appropriate explanation for the tribological behaviour of the tested hydrogels and argued that fluid load support theory for soft, porous materials such as hydrogels have to be reconsidered as evidence is lacking.

- The tested hydrogels were able to sustain low friction without fluid load support, but not under all test conditions. The design of hydrogels as articular cartilage replacements could therefore be improved in terms of their tribological performance by putting more emphasis on the role of surface lubricant in combination with its operating conditions.

Acknowledgements

We would like to thank Tom Welham and Dr Clive Hamer from PCS Instruments for the collaboration in the development of the BioTribometer.

Funding & competing interests

This research did not receive any specific grant from funding agencies in the public, commercial, or not-for-profit sectors.

The authors have no competing interests to declare.

Bibliography

Accardi, M.A., Dini, D., Cann, P.M., 2011. Experimental and numerical investigation of the behaviour of articular cartilage under shear loading - Interstitial fluid pressurisation and lubrication mechanisms. Tribol. Int. 44, 565–578. https://doi.org/10.1016/j.triboint.2010.09.009

Ateshian, G.A., 2009. The role of interstitial fluid pressurization in articular cartilage lubrication. J. Biomech. 42, 1163–1176. https://doi.org/10.1016/j.jbiomech.2009.04.040

Ateshian, G.A., Mow, V.C., 2005. Friction, lubrication, and wear of articular cartilage and diarthrodial joints, in: Basic Orthopaedic Biomechanics and Mechano-Biology. Lippincott Williams & Wilkins, Philadelphia, pp. 447–494.

Ateshian, G.A., Wang, H., Lai, W.M., 1998. The role of interstitial fluid pressurization and surface porosities on the boundary friction of articular cartilage. J. Tribol. 120, 241–248. https://doi.org/10.1115/1.2834416

Baykal, D., Underwood, R.J., Mansmann, K., Marcolongo, M., Kurtz, S.M., 2013. Evaluation of friction properties of hydrogels based on a biphasic cartilage model. J. Mech. Behav. Biomed. Mater. 28, 263–273. https://doi.org/10.1016/j.jmbbm.2013.07.022

Berthe, L., Adams-Chaves, A., Lubrecht, A.A., 2014. Friction measurement indicating the transition between fully flooded and starved regimes in elasto-hydrodynamic lubrication. Proc. Inst. Mech. Eng. Part J J. Eng. Tribol. 228, 1403–1409. https://doi.org/10.1177/1350650114540626

Blum, M.M., Ovaert, T.C., 2013. Low friction hydrogel for articular cartilage repair: Evaluation of mechanical and tribological properties in comparison with natural cartilage tissue. Mater. Sci. Eng. C 33, 4377–4383. https://doi.org/10.1016/j.msec.2013.06.035

Bonnevie, E.D., Baro, V.J., Wang, L., Burris, D.L., 2011. In-situ studies of cartilage microtribology: roles of speed and contact area. Tribol. Lett. 41, 83–95. https://doi.org/10.1007/s11249-010-9687-0

Caligaris, M., Ateshian, G.A., 2008. Effects of sustained interstitial fluid pressurization under migrating contact area, and boundary lubrication by synovial fluid, on cartilage friction. Osteoarthr. Cartil. 16, 1220–1227. https://doi.org/10.1016/j.joca.2008.02.020

Cann, P.M., 1999. Starved grease lubrication of rolling contacts. Tribol. Trans. 42, 867–873. https://doi.org/10.1080/10402009908982294

Cann, P.M.E., Damiens, B., Lubrecht, A.A., 2004. The transition between fully flooded and starved regimes in EHL. Tribol. Int. 37, 859–864. https://doi.org/10.1016/j.triboint.2004.05.005

da Costa Valente, M.L., de Castro, D.T., Macedo, A.P., Shimano, A.C., dos Reis, A.C., 2017. Comparative analysis of stress in a new proposal of dental implants. Mater. Sci. Eng. C 77, 360–365. https://doi.org/10.1016/j.msec.2017.03.268

Damiens, B., Venner, C.H., Cann, P.M.E., Lubrecht, A.A., 2004. Starved Lubrication of Elliptical EHD Contacts. J. Tribol. 126, 105. https://doi.org/10.1115/1.1631020

Daniels, K.E., Kollmer, J.E., Puckett, J.G., 2017. Photoelastic force measurements in granular materials. Rev. Sci. Instrum. 88. https://doi.org/10.1063/1.4983049

Dunn, A.C., Sawyer, W.G., Angelini, T.E., 2014. Gemini interfaces in aqueous lubrication with hydrogels. Tribol. Lett. 54, 59–66. https://doi.org/10.1007/s11249-014-0308-1

Goiato, M.C., de Medeiros, R.A., Sônego, M.V., de Lima, T.M.T., Pesqueira, A.A., dos Santos, D.M., 2017. Stress distribution on short implants with different designs: a photoelastic analysis. J.

Med. Eng. Technol. 41, 115–121. https://doi.org/10.1080/03091902.2016.1239276

Hoffman, A.S., 2002. Hydrogels for biomedical applications. Adv. Drug Deliv. Rev. Deliv. Rev. 54, 3–12. https://doi.org/10.1016/s0169-409x(01)00239-3

Holloway, J.L., Lowman, A.M., Palmese, G.R., 2013. The role of crystallization and phase separation in the formation of physically cross-linked PVA hydrogels. Soft Matter 9, 826–833. https://doi.org/10.1039/c2sm26763b

Holloway, J.L., Lowman, A.M., Palmese, G.R., 2010. Mechanical evaluation of poly(vinyl alcohol)-based fibrous composites as biomaterials for meniscal tissue replacement. Acta Biomater. 6, 4716–4724. https://doi.org/10.1016/j.actbio.2010.06.025

Hou, Y., Chen, C., Liu, K., Tu, Y., Zhang, L., Li, Y., 2015. Preperation of PVA hydrogel with high-transparence and investigations of its transparent mechanism. RSC Adv. 5, 24023–24030. https://doi.org/10.1039/c5ra01280e

Hyon, S.H., Cha, W.I., Ikada, Y., 1989. Preparation of transparant poly(vinyl alcohol) hydrogel. Polym. Bull. 22, 119–122.

Jahn, S., Seror, J., Klein, J., 2016. Lubrication of Articular Cartilage. Annu. Rev. Biomed. Eng. 18, 235–258. https://doi.org/10.1146/annurev-bioeng-081514-123305

Kaneta, M., Todoroki, H., Nishikawa, H., Kanzaki, Y., Kawahara, Y., 2000. Tribology of flexible seals for reciprocating motion. J. Tribol. 122, 787–795. https://doi.org/10.1115/1.1310573

Kita, M., Ogura, Y., Honda, Y., Suong-Hyu Hyon, 1990. Evaluation of polyvinyl alcohol hydrogel as a soft contact lens material. Graefe´s Arch Clin Exp Ophtalmol 228, 533–537. https://doi.org/10.1007/BF00918486

Krishnan, R., Kopacz, M., Ateshian, G.A., 2004. Experimental verification of the role of interstitial fluid pressurization in cartilage lubrication. J. Orthop. Res. 22, 565–570. https://doi.org/10.1016/j.orthres.2003.07.002

Kuske, A., Robertson, G., 1974. Photoelastic stress analysis. John Wiley & Sons.

Li, F., Su, Y., Wang, J., Wu, G., Wang, C., 2010. Influence of dynamic load on friction behavior of human articular cartilage, stainless steel and polyvinyl alcohol hydrogel as artificial cartilage. J. Mater. Sci. Mater. Med. 21, 147–154. https://doi.org/10.1007/s10856-009-3863-5

Majda, D., Bhattarai, A., Riikonen, J., Napruszewska, B.D., Zimowska, M., Michalik-Zym, A., Töyräs, J., Lehto, V.P., 2017. New approach for determining cartilage pore size distribution: NaCl-thermoporometry. Microporous Mesoporous Mater. 241, 238–245. https://doi.org/10.1016/j.micromeso.2017.01.005

Majmudar, T.S., Behringer, R.P., 2005. Contact force measurements and stress-induced anisotropy in granular materials. Nature 435, 1079–1082. https://doi.org/10.1038/nature03805

McCutchen, C.W., 1962. The frictional properties of animal joints. Wear 5, 1–17. https://doi.org/10.1016/0043-1648(62)90176-x

McCutchen, C.W., 1959. Mechanism of animal joints: Sponge-hydrostatic and weeping bearings. Nature 184, 1284–1285. https://doi.org/10.1038/1841284a0

Milner, P.E., Parkes, M., Puetzer, J.L., Chapman, R., Stevens, M.M., Cann, P., Jeffers, J.R.T., 2018. A low friction, biphasic and boundary lubricating hydrogel for cartilage replacement. Acta Biomater. 65, 102–111. https://doi.org/10.1016/j.actbio.2017.11.002

Moore, A.C., Burris, D.L., 2017. Tribological rehydration of cartilage and its potential role in preserving joint health. Osteoarthr. Cartil. 25, 99–107. https://doi.org/10.1016/j.joca.2016.09.018

Moore, A.C., Burris, D.L., 2014. An analytical model to predict interstitial lubrication of cartilage in migrating contact areas. J. Biomech. 47, 148–153. https://doi.org/10.1016/j.jbiomech.2013.09.020

Mow, V.C., Ratcliffe, A., Poole, A.R., 1992. Cartilage and diarthrodial joints as paradigms for hierarchical materials and structures. Biomaterials 13, 67–97. https://doi.org/10.1016/0142-9612(92)90001-5

Mow, V.C., Yong Gu, W., Hui Chen, F., 2005. Composition and structure of articular cartilage and meniscus, in: Mow, V.C., Huiskes, R. (Eds.), Basic Orthopaedic Biomechanics and Mechano-Biology. Lippincott Williams & Wilkins, Philadelphia, pp. 185–198.

Murakami, T., Ohtsuki, N., Higaki, H., 1993. The adaptive multimode lubrication in knee prostheses with compliant layer during walking motion. Tribol. Ser. 25, 673–682. https://doi.org/10.1016/S0167-8922(08)70420-6

Murakami, T., Sakai, N., Yamaguchi, T., Yarimitsu, S., Nakashima, K., Sawae, Y., Suzuki, A., 2015. Evaluation of a superior lubrication mechanism with biphasic hydrogels for artificial cartilage. Tribiology Int. 89, 19–26. https://doi.org/10.1016/j.triboint.2014.12.013

Murakami, T., Yarimitsu, S., Nakashima, K., Yamaguchi, T., Sawae, Y., Sakai, N., Suzuki, A., 2014. Superior lubricity in articular cartilage and artificial hydrogel cartilage. Proc. Inst. Mech. Eng. Part J 228, 1099–1111. https://doi.org/10.1177/1350650114530273

O'Connell, G.D., Lima, E.G., Bian, L., Chahine, N.O., Albro, M.B., Cook, J.L., Ateshian, G.A., Hung, C.T., 2012. Toward engineering a biological joint replacement. J. Knee Surg. 25, 187–196. https://doi.org/10.1055/s-0032-1319783

Park, S., Krishnan, R., Nicoll, S.B., Ateshian, G.A., 2003. Cartilage interstitial fluid load support in unconfined compression. J. Biomech. 36, 1785–1796. https://doi.org/10.1016/S0021-9290(03)00231-8

Parkes, M., Myant, C., Dini, D., Cann, P., 2015. Tribology-optimised silk protein hydrogels for articular cartilage repair. Tribol. Int. 89, 9–18. https://doi.org/10.1016/j.triboint.2014.11.024

Peppas, N.A., 1975. Turbidimetric studies of aqueous poly(vinyl alcohol) solutions. Makromol. Chemie 176, 3433–3440. https://doi.org/10.1002/macp.1975.021761125

Pitenis, A.A., Urueña, J.M., Schulze, K.D., Nixon, R.M., Dunn, A.C., Krick, B.A., Sawyer, W.G., Angelini, T.E., 2014. Polymer fluctuation lubrication in hydrogel gemini interfaces. Soft Matter 10, 8955–8962. https://doi.org/10.1039/C4SM01728E

Schulze, K.D., Hart, S.M., Marshall, S.L., O'Bryan, C.S., Urueña, J.M., Pitenis, A.A., Sawyer, W.G., Angelini, T.E., 2017. Polymer osmotic pressure in hydrogel contact mechanics. Biotribology 11, 3–7. https://doi.org/10.1016/j.biotri.2017.03.004

Shukla, A., Dally, J.W., 2014. Optical methods of stress, strain and discplacement analysis, in: Experimental Solid Mechanics. College House Enterprises, LLC., Knoxville, pp. 259–509.

Silva, M., Shepherd, E.F., Jackson, W.O., Dorey, F.J., Schmalzried, T.P., 2002. Average patient walking activity approaches 2 million cycles per year: Pedometers under-record walking activity. J. Arthroplasty 17, 693–697. https://doi.org/10.1054/arth.2002.32699

Spiller, K.L., Maher, S.A., Lowman, A.M., 2011. Hydrogels for the repair of articular cartilage defects.

Tissue Eng. Part B 17, 281–299. https://doi.org/10.1089/ten.teb.2011.0077

Stammen, J.A., Williams, S., Ku, D.N., Guldberg, R.E., 2001. Mechanical properties of a novel PVA hydrogel in shear and unconfined compression. Biomaterials 22, 799–806. https://doi.org/10.1016/S0142-9612(00)00242-8

Stewart, T., Jin, Z.M., Fisher, J., 1997. Friction of composite cushion bearings for total knee joint replacements under adverse lubrication conditions. Proc. Inst. Mech. Eng. Part H 211, 451–465. https://doi.org/10.1243/0954411981534574

Tomlinson, R.A., Taylor, Z.A., 2015. Photoelastic materials and methods for tissue biomechanics applications. Opt. Eng. 54, 1–9. https://doi.org/10.1117/1.oe.54.8.081208

Walker, P.S., Dowson, D., Longfield, M.D., Wright, V., 1968. "Boosted lubrication" in synovial joints by fluid entrapment and enrichment. Ann. Rheum. Dis. 27, 512–520. https://doi.org/10.1136/ard.27.6.512

Wang, G., Huang, W., Song, Q., Liang, J., 2017. Three-dimensional finite analysis of acetabular contact pressure and contact area during normal walking. Asian J. Surg. 40, 463–469. https://doi.org/10.1016/j.asjsur.2016.07.002

Wedeven, L.D., Evans, D., Cameron, A., 1971. Optical Analysis of Ball Bearing Starvation. J. Lubr. Technol. 93, 349–361. https://doi.org/10.1115/1.3451591